Observing the SO2 and Sulfate Aerosol Plumes From the 2022 Hunga Eruption With the Infrared Atmospheric Sounding Interferometer (IASI)

Pasquale Sellitto, Richard Siddans, Redha Belhadji, Elisa Carboni, Bernard Legras, Aurélien Podglajen, Clair Duchamp, Brian Kerridge

Geophysical Research Letters

RESEARCH LETTER
10.1029/2023GL105565

Key Points:

- Novel co-retrieval of SO_2 and sulfate aerosol from Infrared Atmospheric Sounding Interferometer (IASI) used to study the dispersion of the Hunga plume over the entire year 2022
- Rapid conversion of SO_2 (2 weeks e-folding time) and long-lasting sulfate aerosol observed
- Larger SO_2 injected mass burden (>1.0 Tg) than previously thought and a large sulfate aerosol total burden (1.6 Tg) estimated

Supporting Information:

Supporting Information may be found in the online version of this article.

Correspondence to:

P. Sellitto,
pasquale.sellitto@lisa.ipsl.fr

Citation:

Sellitto, P., Siddans, R., Belhadji, R., Carboni, E., Legras, B., Podglajen, A., et al. (2024). Observing the SO_2 and sulfate aerosol plumes from the 2022 Hunga eruption with the Infrared Atmospheric Sounding Interferometer (IASI). *Geophysical Research Letters*, *51*, e2023GL105565. https://doi.org/10.1029/2023GL105565

Received 19 JUL 2023
Accepted 23 JUL 2024

Observing the SO_2 and Sulfate Aerosol Plumes From the 2022 Hunga Eruption With the Infrared Atmospheric Sounding Interferometer (IASI)

Pasquale Sellitto[1,2], Richard Siddans[3,4], Redha Belhadji[1], Elisa Carboni[3,4], Bernard Legras[5], Aurélien Podglajen[5], Clair Duchamp[5], and Brian Kerridge[3,4]

[1]Univ Paris Est Creteil and Université Paris Cité, CNRS, LISA, Créteil, France, [2]Istituto Nazionale di Geofisica e Vulcanologia, Osservatorio Etneo, Catania, Italy, [3]National Centre for Earth Observation, STFC Rutherford Appleton Laboratory, Chilton, UK, [4]Remote Sensing Group, STFC Rutherford Appleton Laboratory, Chilton, UK, [5]Laboratoire de Météorologie Dynamique (LMD-IPSL), CNRS, Sorbonne Université, ENS-PSL, École Polytechnique, Paris, France

Abstract The Hunga volcano violently erupted on 15 January 2022, producing the largest perturbation of the stratospheric aerosol layer since Pinatubo 1991, despite the initially estimated modest injection of SO_2. This study presents novel SO_2 and sulfate aerosol (SA) co-retrievals from the Infrared Atmospheric Sounding Interferometer, and uses them to quantify the initial progression of the Hunga plume. These observations are consistent with rapid conversion of SO_2 (e-folding time: 17.1 ± 4.3 days) to SA, with an injected burden of >1.0 Tg SO_2. This points at larger SO_2 injections than previously thought. A long-lasting SA plume was observed, with two separate build-up phases, and with a meridional dispersion of marked anomalies from the tropics to the higher southern hemispheric latitudes. A limited (∼20%) SA removal was observed after 1-year dispersion. The total injected SA mass burden was estimated at 1.6 ± 0.5 Tg in the total atmospheric column, with a build-up e-folding time of about 2 months.

Plain Language Summary The eruption of the submarine Hunga volcano in January 2022 polluted the global stratosphere with a large amount of water vapor and significantly perturbed the stratospheric aerosol layer. In this paper, we present a 1-year long aftermath study of the stratospheric sulfur pollution from this volcanic eruption using observations from the Infrared Atmospheric Sounding Interferometer (IASI) satellite-borne instrument. Gaseous and aerosol sulfur emissions are observed simultaneously using the specific potential of this sensor. These observations provide unique capabilities to characterize the aerosol type in the Hunga plume and the sulfur cycle associated with the volcanic emissions. An extremely rapid conversion of gaseous sulfur emissions to aerosols is observed, leading to larger than expected and persistent anomalies of the stratospheric aerosol layer (compared with a consistent long-term climatology), still noticeable in the Southern Hemisphere after 1 year. The total mass of the emitted sulfur in gas and aerosol state is also simultaneously estimated, for the first time.

1. Introduction

After about a month of volcanic unrest, the Hunga volcano (Kingdom of Tonga) violently erupted on 15 January 2022, with a Volcanic Explosivity Index (VEI) of ∼6 (Poli & Shapiro, 2022). The shallow submarine volcanic setting of Hunga produced a phreato-Plinian eruption plume, with an injection at very high altitude, reaching up to 55 km (Carr et al., 2022), and an unprecedented amount of ∼140 Tg (10% of the overall stratospheric content) of stratospheric water vapor (Khaykin et al., 2022; Millàn et al., 2022). Due to the extremely high concentrations of water vapor within the Hunga plume, extremely fast conversion of volcanic sulfur dioxide (SO_2) to sulfate aerosols (SA) was observed (Sellitto et al., 2022; Vernier et al., 2022) and explained with modeling studies (∼28 days e-folding time in Zhu et al., 2022). After a few days, the stratospheric aerosol perturbations by the Hunga eruption could be attributed solely to SA, without any optical signature of ash (Sellitto et al., 2022). Small liquid spherical droplets, consistent with SA, were also observed with balloon-borne in situ optical counter measurements during a rapid response campaign at La Réunion island, in the south-western Indian Ocean (Kloss et al., 2022). The Hunga water vapor and SA plumes circumnavigated the Earth in the two following weeks and then dispersed over the Southern Hemisphere (Khaykin et al., 2022; Legras et al., 2022; Sellitto et al., 2022). Besides the exceptional large-scale enhancement in stratospheric water vapor, the Hunga eruption proved to be the largest perturbation in the stratospheric aerosol layer for 30 years, in particular in the tropics and Southern

Hemisphere (Khaykin et al., 2022; Sellitto et al., 2022). This was somewhat surprising because of the limited SO_2 emissions associated with this event, based on first estimations with satellite observations (0.4–0.5 Tg for the main event of 15 January and 0.6–0.7 Tg for the overall eruptive activity, Carn et al., 2022). Despite this significant SA perturbations of the stratospheric aerosol layer, the Hunga plume was associated with an uncommon climate warming effect, due to the large amount of the water vapor perturbations and its infrared radiative emission effect (Sellitto et al., 2022). The Hunga plume radiative effect is also associated with a stratospheric cooling (Coy et al., 2022; Schoeberl et al., 2022; Vömel et al., 2022), a radiatively-driven descent (Sellitto et al., 2022) and a likely detrimental effect on the target of keeping the anthropogenic global warming at 1.5°C in 2030 (Forster et al., 2023; Jenkins et al., 2023).

In this paper, we use novel simultaneous SO_2 and SA observations from the high-spectral-resolution infrared space-borne instrument IASI (Infrared Atmospheric Sounding Instrument) to study the SO_2 and SA plume dispersion more than 1 year after the Hunga eruption and to re-estimate their injected burdens, extending the first results presented by Sellitto et al. (2022).

2. Data and Methods

2.1. SO_2 and SA Observations With IASI Using the RAL IMS Scheme

The RAL (Rutherford Appleton Laboratory) Infrared/Microwave Sounder (IMS) retrieval core scheme (Siddans, 2019) uses an optimal estimation spectral fitting procedure to retrieve atmospheric and surface parameters jointly from co-located measurements by IASI (Infrared Atmospheric Sounding Interferometer), AMSU (Advanced Microwave Sounding Unit) and MHS (Microwave Humidity Sounder) on MetOp-B spacecraft, using RTTOV-12 (Radiative Transfer for TOVS) (Saunders et al., 2017) as the forward radiative transfer model. The use of RTTOV-12 enables the quantitative retrieval of volcanic-specific aerosols (SA) and trace gases (SO_2). The present paper uses IMS SO_2 and SA observations from its near-real-time implementation. The IMS scheme retrieves the SO_2 concentration in the sensitive region around 1,100–1,200 cm^{-1} assuming a uniform vertical mixing ratio profile. It retrieves sulfate-specific optical depth at 1,170 cm^{-1} (8.5 μm) (i.e., the peak of SA mid-infrared extinction cross section; Sellitto & Legras, 2016), assuming a Gaussian extinction coefficient profile shape peaking at 20 km altitude, with 2 km full-width half-maximum. The bulk of the spectroscopic information on SO_2 and SA, in the IMS scheme, thus comes from IASI (Clerbaux et al., 2009). The IMS scheme simultaneously retrieves SO_2 and SA spectroscopic information, which is crucial to avoid the very large uncertainties on both due to their co-existence in volcanic plume and overlapping spectral signatures (Sellitto et al., 2019). On the contrary, the weaker SA band at ∼900 cm^{-1} (11.1 μm) should be used in case of exclusive SA retrievals, thus with larger uncertainties due to smaller signal-to-noise ratio with respect to the more intense 1,170 cm^{-1} band (Guermazi et al., 2021). At present, the RAL IMS scheme is the only available method that co-retrieves the two species, thus allowing the use of the stronger 1,170 cm^{-1} band and the minimization of the cross-biases in SO_2 and SA retrievals. Total uncertainties of individual IMS SO_2 and SA retrievals are estimated at 0.3 DU (SO_2) and 0.002 (SA optical depth) (Siddans, 2023). Due to assumptions on the Hunga SO_2 and SA plumes vertical profiles in the IMS scheme, an additional 10% systematic uncertainty has been added. The IMS and SO_2 retrievals are scarcely sensitive to the assumed altitude, in the range 20–30 km (Siddans, 2023). More information on the vertical sensitivity of the IMS scheme is in the Text S1 in Supporting Information S1. The novel IMS SA optical depth observations have been found consistent with CALIOP (Cloud-Aerosol Lidar with Orthogonal Polarization) space LiDAR and OMPS (Ozone Mapping and Profiler Suite Limb Profiler) limb instrument (Legras et al., 2022). We refer to the SA optical depth at 1170 cm^{-1} as SA OD in this work. The data are provided daily on a regular grid with 0.25° resolution in latitude and longitude, collecting both the daytime and nighttime swaths. In this paper, averages and percentiles over the period 2007–2018 are provided as climatological reference (i.e., including tropospheric SA variability but also all perturbing effects like the previous moderate eruptions in the life time of IASI), and are compared with observation for the full year 2022. Note that the climatological reference is obtained with MetOp-A IASI data. Anomalies associated with the 2022 Hunga eruption are defined as the observations in 2022 minus the 2007–2018 climatology.

2.2. SO_2 and SA Total Mass Burden Estimation

The total mass burden of SO_2 and SA (M_{SO2} and M_{SA}) from Hunga eruption are obtained with IMS/IASI co-retrievals, considering the latitude interval between the 10°N and 70°S and subtracting a baseline burden

before the eruption signature. For short-term analyses of SO_2 rapid conversion, this baseline was taken as the conditions before the eruption (on 13th January), while for the 1-year SA analysis, the SA OD anomaly is considered (thus climatological baseline is subtracted out).

While the calculation of the SO_2 mass burden is straightforward, assumptions on some chemical and physical properties of the SA particles are needed to estimate the SA mass burden (Sellitto & Legras, 2016). The SA mass burden is calculated using the following equation:

$$M_{SA} = \text{SA OD}/\langle \text{MEE} \rangle \quad (1)$$

An average mid-infrared mass aerosol extinction efficiency (⟨MEE⟩) centered around the peak SA absorption band at 1,170 cm^{-1} (8.5 μm) is obtained with the Oxford Mie routines (available at the following website: http://eodg.atm.ox.ac.uk/MIE/) and using Equation 2. This equation is based on the derivation of Clyne et al. (2021), adapted to the mid-infrared and using a particle number size distribution (particle mass size distribution is used in Clyne et al., 2021).

$$\langle \text{MEE} \rangle = \frac{3}{4 * \rho_p * r_{\text{eff}}} * Q_{\text{ext}}(r_m) \quad (2)$$

In Equation 2, ρ_p is the SA average mass density taken as 1.75 g cm^{-3} (a typical value for a sulfuric acid percent weight 70% and lower-stratospheric temperatures, see Duchamp et al., 2023), r_{eff} is the effective radius of the SA particles and Q_{ext} is the extinction efficiency factor calculated with the Mie code, using SA complex refractive index from Biermann et al. (2000). The MEE depends critically on the particles mean size (r_{eff} and r_m) and size distribution width (σ). Duchamp et al. (2023) estimated, with limb satellite observations, that typical r_{eff} for the Hunga plume core are in the range 0.35–0.45 μm and a typical σ is 1.25, while smaller mean particle size (r_{eff} down to ∼0.25 μm) and larger width (σ up to 1.8) can be found in more vertically- and latitudinally-peripheric plumes sections. Using these different values we obtain a large range of ⟨MEE⟩, between ∼0.20 and ∼0.45 m^2g^{-1}, mostly dependent on the assumption on σ. Averaging all these values, we obtain a ⟨MEE⟩ 0.33 m^2g^{-1}. Due to this large variability of ⟨MEE⟩, the SA total mass burden systematic uncertainties associated with the SA size distribution assumption, and transferred to the SA mass from the ⟨MEE⟩ selected value, are chosen at a 35% value in this work. Smaller systematic uncertainties can be associated with the assumption of ρ_p (an additional 10% value has been chosen).

3. Results

3.1. SO_2 and SA Anomalies Induced by the Hunga Eruption at the Hemispheric Scale

Legras et al. (2022) and Sellitto et al. (2022) (see e.g., Figure 3a of this latter paper) observed the rapid conversion of the SO_2 emission from Hunga eruption to SA. Detections of SO_2 exceeding a relatively small threshold (2 DU) are not visible from IASI observations after the end of January, that is, about 2 weeks after the eruption (Figure S1 in Supporting Information S1). Since February 2022, SA dominate the sulfur plume and must be used to study its dispersion at the hemispheric scale at longer timescales than a few weeks. Figure 1a shows the monthly mean SA OD anomaly for the year 2022 (monthly mean absolute SA OD retrievals are in Figure S2 in Supporting Information S1). A distinct anomaly in SA OD due to the Hunga eruption, reaching values larger than 0.005 in February/March can be seen. The SA OD anomaly is initially located in the latitude band between 0 and 25°S, where the Hunga volcano is located, and then progressively spreads toward southern hemispheric mid-latitudes and high-latitudes, after June 2022. The SA OD anomalies appear longitudinally well mixed since February, thus supporting the evidence of a rapid initial circumnavigation of the Earth, as reported by Legras et al. (2022) and Khaykin et al. (2022). The zonal transport of the Hunga plume is quicker than what observed for recent moderate eruptions, like Nabro 2011 (circumnavigation in ∼2 months, Bourassa et al., 2012) and Raikoke 2019 (∼1 month, Kloss et al., 2021). The meridional dispersion dynamics of the Hunga plume can be seen in a compact manner with SA OD anomalies zonal means in Figure 1b. In contrast with the zonal transport, meridional dispersion at the southern hemispheric scale is significantly slower that for recent moderate stratospheric eruptions. While early detections at southern and northern hemispheric locations were associated with detached plumes filaments (Khaykin et al., 2022; Taha et al., 2022), the Hunga plume systematically reached high-latitudes after 6 months

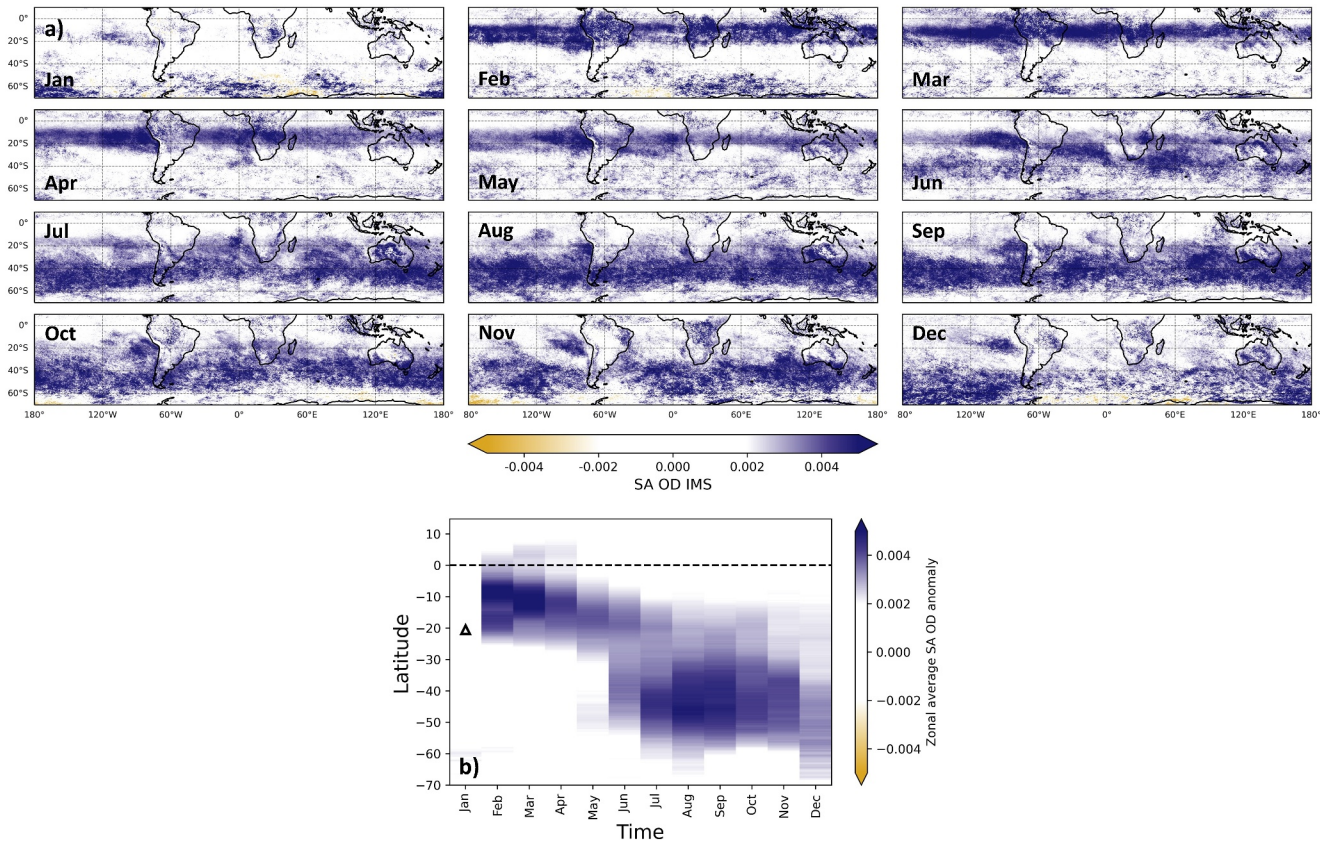

Figure 1. (a) Monthly mean SA OD (at 8.5 μm) anomaly from IASI observations in 2022, from 10°N to 70°S. (b) Zonal average SA OD anomaly from IASI observations in 2022, in the same latitude range as panel (a). The month/latitude position of the Hunga eruption is indicated as a black triangle.

(Figure 1). The Hunga plume crossed only marginally the equator and the northern hemispheric stratospheric aerosol layer is not significantly perturbed by this event (see also Figure 3e in Sellitto et al., 2022). Two distinct phases in the build-up of the SA plume seem to appear, one in February/March at 10–20°S and one in July/August at 30–50°S. This second late build-up phase, which was also observed by SAGE III/ISS (Duchamp et al., 2023) and OMPS-LP (Text S2, Figure S3 in Supporting Information S1), is still to be fully understood and studies are ongoing.

The spatiotemporal propagation of the SA OD perturbations discussed above can also be seen by directly comparing zonal average values of the SA OD in 2022 and for the 2007–2018 climatology (Figure S4 in Supporting Information S1). While a perturbation is not clearly visible in January, a pronounced perturbation, largely exceeding the 5–95 percentile interval of climatology, appears in February between the equator and 30°S and then spreads gradually to higher latitudes in the Southern Hemisphere. Figure 2 shows average values in selected latitude regional bands. The Northern Hemisphere does not look affected by the Hunga eruption throughout the year 2022 (a perturbation during the first months of 2022 can be seen at northern hemispheric mid-latitudes but seems unrelated with the Hunga eruption). Very large perturbations can be seen since January in the tropics and since March–April in southern hemispheric mid-latitudes. A limited perturbation is also visible since April for southern hemispheric high-latitudes. The whole Southern Hemisphere is still perturbed by December 2022, except for very high latitudes.

3.2. The Sulfur Cycle in the Hunga Plume

Figures 3a and 3b show the short-term (from the eruption to late February) evolution of the estimated SO_2 and SA total mass burdens. For almost instantaneous explosive events like Hunga eruption, the SO_2 mass burden is expected to reach its maximum in the very first days and then exponentially decrease due to chemical sink associated with the conversion to SA, as described in Equation 3.

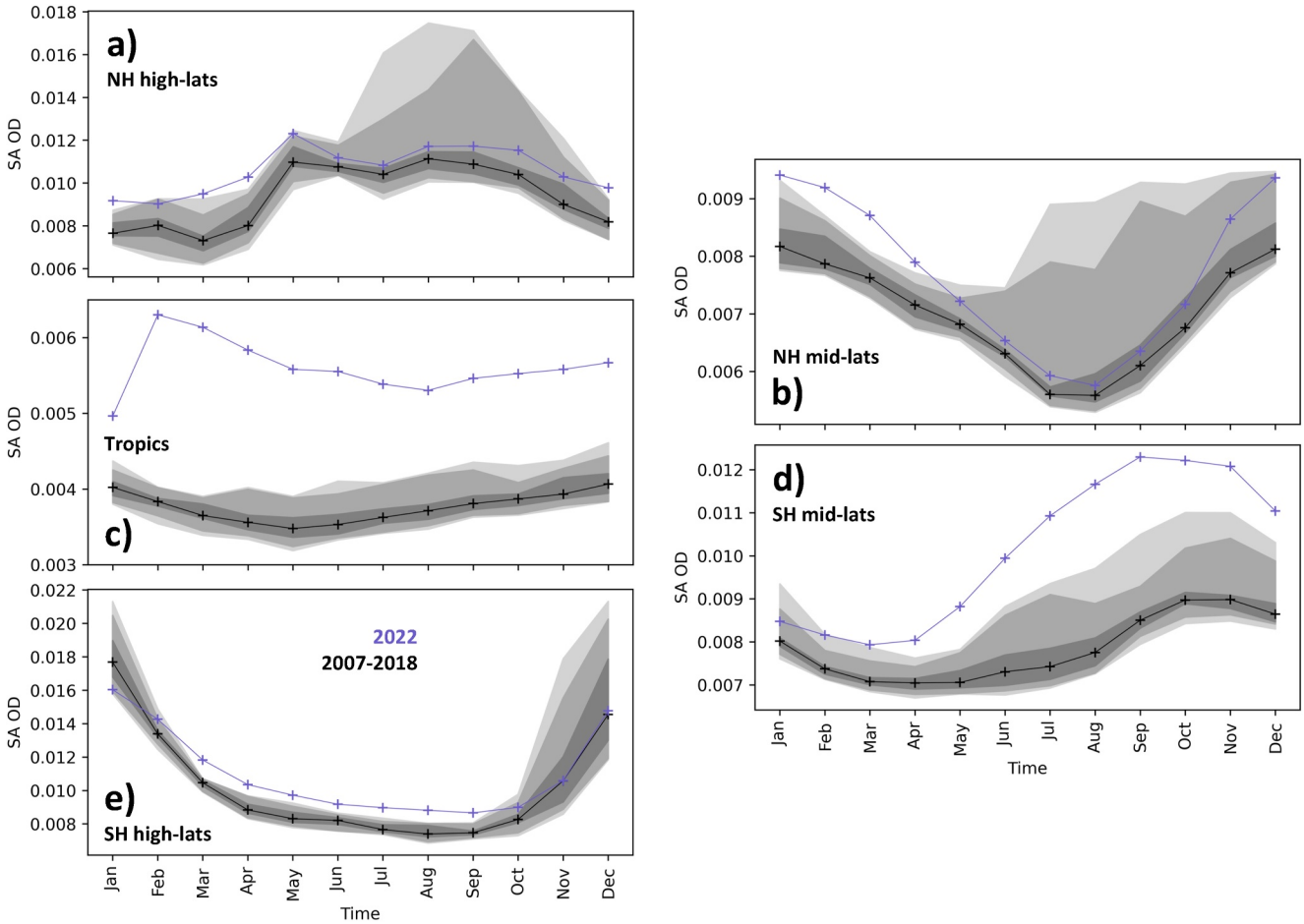

Figure 2. Regional monthly mean IASI SA OD in 2022 (blue lines and crosses), and median values (black lines and crosses), 5–95 (dark gray shaded area), 10–90 (medium gray shaded area) and 30–70 (light gray shaded area) percentiles intervals for the period 2007–2018, in the five latitude regions: northern hemispheric high-latitudes (60°N–90°N, panel (a)), northern hemispheric mid-latitudes (30°N–60°N, panel (b)), tropics (30°N–30°S, panel (c)), southern hemispheric mid-latitudes (30°S–60°S, panel (d)) and southern hemispheric high-latitudes (60°S–90°S, panel (e)).

$$M_{SO2}(t) = M_{SO2}(t_0) * e^{-\frac{t}{\tau_{SO2}}} \quad (3)$$

In Equation 3, $M_{SO2}(t)$ and $M_{SO2}(t_0)$ are the mass burden at a given time and the total mass burden injected at the time of the eruption, and τ_{SO2} is the e-folding time due to chemical conversion to SA. A surprising feature of the IASI-estimated Hunga SO_2 mass burden evolution is that a clear maximum is not observed immediately after the eruption but a few days later, that is, on 19 January (Figure 3a). The total mass burden on 15 January is about 0.45 Tg, very close to the initial SO_2 mass burden estimation of Carn et al. (2022) with Sentinel-5p TROPOMI (TROPOspheric Monitor Instrument), which is the present reference of the injected SO_2 from the Hunga eruption. The larger values in the days after the eruption, reaching values as large as 1.0 Tg, might point at an initial underestimation of the SO_2 total injected mass burden, possibly due to ash- or water-vapor-induced opacity of the very young plume. The IASI observations suggest that the injected SO_2 mass burden of the Hunga eruption could be larger than previously thought, with a 1.0 Tg SO_2 (~0.5 Tg S) lower limit. A parameterized exponential decay function, as the one of Equation 3, fitted to the SO_2 mass burden data (starting from 18 January, see Figure 3a) obtained an injected SO_2 mass of 1.0 ± 0.2 Tg and an e-folding time of 17.1 ± 4.3 days (see Table 1). This latter value suggests a 2-to-3 times faster chemical sink due to conversion to SA than expected at the Hunga plume's altitudes (e.g., Carn et al., 2016), and even quicker than the ~28 days e-folding time estimated for Hunga with modeling studies by Zhu et al. (2022). The fast conversion to SA is a known feature of the Hunga plume,

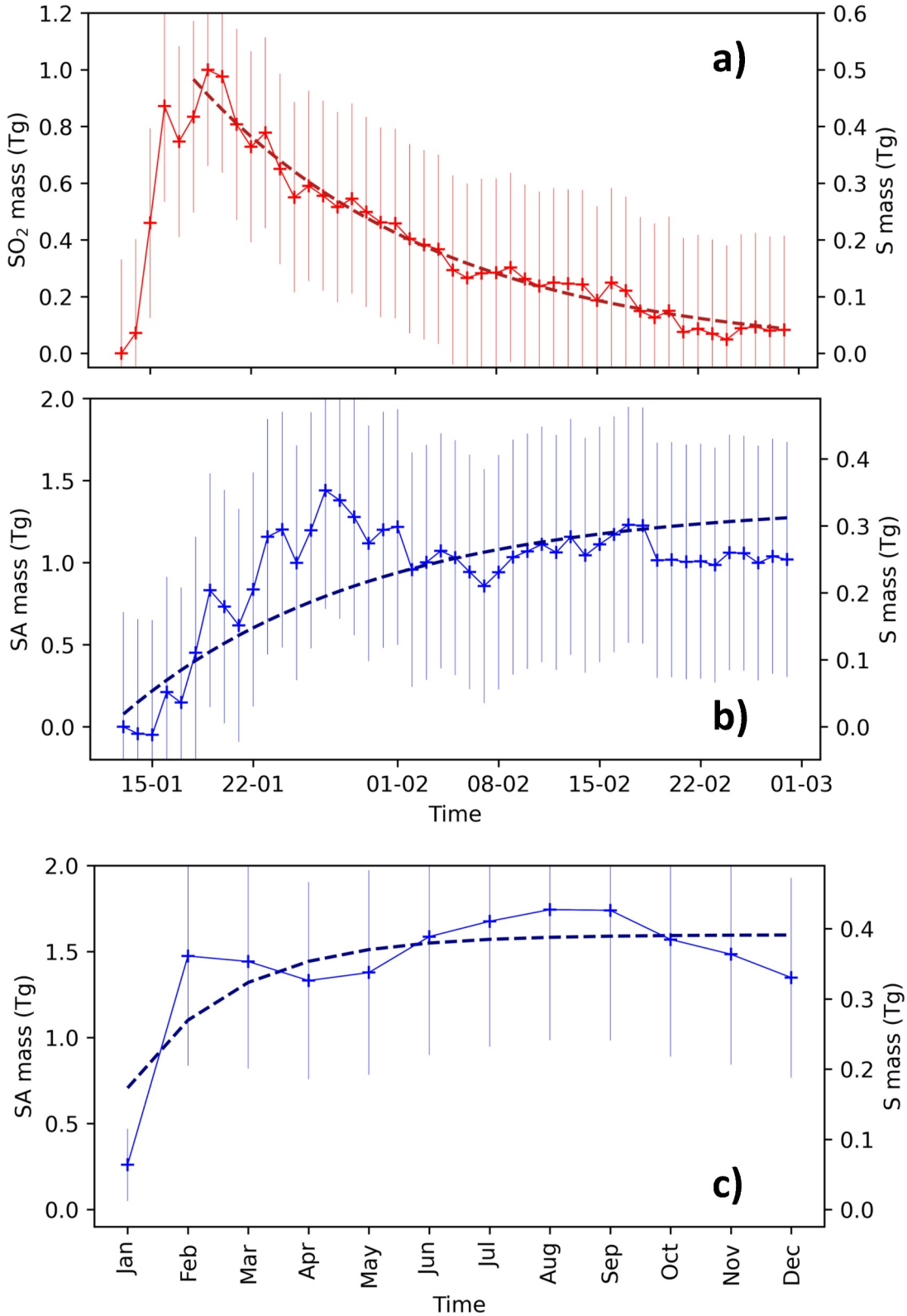

Figure 3. (a, b) Short term (January and February 2022) temporal evolution of SO_2 (panel a) and SA (panel b) total anomaly masses due to the Hunga eruption, estimated using daily average IASI SO_2 total column and SA OD observations. (c) Long term (year 2022) temporal evolution of SA total anomaly mass due to the Hunga eruption, estimated using monthly average IASI SA OD observations. In panels (a–c), fit of parameterization functions of the total masses evolution is also shown, see text for more details (sampled at the end of each month for Figure 3c). The total sulfur (S) mass is indicated for both SO_2 and SA in panels a–c.

Table 1
Estimated SO_2 and SA Total Injected Masses (M_{SO2} and M_{SA}, Respectively), SO_2 Decay e-Folding Time (τ_{SO2}) and SA Build-Up e-Folding Time (τ_{SA}), Based on the Parameterization of Equation 3 (M_{SO2} and τ_{SO2}) and Equation 4 (M_{SA} and τ_{SA}) Shown in Figures 3a and 3c

M_{SO2}	1.0 ± 0.2 Tg
τ_{SO2}	17.1 ± 4.3 days
M_{SA}	1.6 ± 0.5 Tg
τ_{SA}	52.7 ± 12.4 days

attributed to the large amount of water vapor due to the phreatic nature of this event (e.g., Sellitto et al., 2022; Zhu et al., 2022).

Figure 3c shows the temporal evolution of the SA mass during the whole year 2022. The SA plume build-up is modeled by the exponential function of Equation 4, where $M_{SA}(t)$ and $M_{SA}(t_\infty)$ are the SA mass burden at a given time and the total SA mass burden after full build-up of the plume, and τ_{SA} is the build-up e-folding time. Equation 4 assumes that SA sinks (gravitational settling, evaporation and others) are not effective at the 1-year time scale.

$$M_{SA}(t) = M_{SA}(t_\infty) * \left(1 - e^{-\frac{t}{\tau_{SA}}}\right) \quad (4)$$

Fitting Equation 4 to the SA mass burden data estimated from the SA observations (Figure 3c), we obtain that, after an e-folding build-up time of 52.7 ± 12.4 days, that is, ∼2 months, an anomalous SA mass burden of 1.6 ± 0.5 Tg (∼0.4 Tg S) is reached (see Table 1). Sellitto et al. (2022) proposed a range of values between 1.0 and 3.0 Tg for the injected SA mass burden, depending on the particles size. There is now increasing consensus that the effective radius of the Hunga aerosol plume does not exceed 0.5 μm (e.g., Duchamp et al., 2023), which reduces uncertainties on the MEE (see Section 2.2) and places the SA mass burden in the middle of that previous range. Using limb-satellite SAGE III/ISS observations, Duchamp et al. (2023) estimated the stratospheric H_2SO_4 total mass at a maximum of ∼0.7 Tg which corresponds, with the assumption of a H_2SO_4 weight percentage of 70%, to a stratospheric SA mass of ∼1.0 Tg. Our present estimate is obtained with a nadir-viewing instrument and is representative of the total tropospheric-plus-stratospheric column. To compare the two estimates, we made a crude estimation of the proportion of Hunga aerosols in the troposphere and stratosphere using OMPS data (Figure S5 in Supporting Information S1). Taking for example, zonal average AOD observations in March (Figure S5d in Supporting Information S1), we estimate that ∼40–50% of the total column aerosols are in the stratosphere. With this assumption, our IASI SA mass burden distributes as ∼0.80–0.95 Tg in the troposphere and ∼0.65–0.80 Tg in the stratosphere. This latter value is consistent with SAGE III/ISS estimations of Duchamp et al. (2023), even if slightly smaller. It is worth noting that the OMPS-based repartition of SA in troposphere and stratosphere is very crude, in particular due the possibility of cloud contamination in the troposphere, so this has to be taken with caution. In general, a 1.0 Tg mass burden of SO_2, if totally converted to SA with 70% H_2SO_4 weight percentage would lead to ∼2.2 Tg of SA. Thus, our 1.6 Tg SA mass burden estimate points at a ∼30% lower values than in case of full SO_2 conversion to SA, based on our SO_2 mass estimation. While these deviations are still limited when compared with the uncertainty budget of our SO_2 and SA mass estimations, possible issues with IASI SA OD sensitivity or to an additional sink for SO_2 or SA cannot be excluded at this stage.

It is interesting to notice that the two distinct build-up phases of the SA plume discussed in Sect. 3.1 in terms of the SA OD are also visible in the SA mass burden evolution (Figures 3b and 3c, see maxima in January-February and in August). This latter evidence excludes the possibility that this effect is due merely to meridional transport.

The SA mass burden in December 2022 is about 1.3 Tg, thus pointing at a limited (20%) SA removal during the year 2022. The removal of stratospheric SA was about twice as fast for Pinatubo (e.g., Sukhodolov et al., 2018 and references therein).

Using these novel AOD estimations in the thermal infrared in combination with total column AOD observations in the visible spectral range of for example, OMPS-LP (Figure S5 in Supporting Information S1), a shortwave-to-longwave average Ångström Exponent (AE) can be estimated. For the month of March 2022, when the first build-up phase of the plume is almost completed, we obtain visible and infrared AODs of 0.044 and 0.0026, thus with an AE of 1.13 (Table S1 in Supporting Information S1). Similar values of the AE were obtained in the visible range alone by Taha et al. (2022).

4. Conclusions

In this paper, we have presented novel IASI SO_2/SA co-retrievals, that were used to track and analyze the sulfur plume emanated from the record-breaking Hunga eruption of 15 January 2022. The full year 2022 of retrievals is used here. We observed a rapid conversion of SO_2 to SA, with an estimated e-folding time of 17.1 ± 4.3 days—a clear SO_2 signal is not observable since February 2022. We estimated a lower limit 1.0 Tg for the initial injected

SO_2 burden, which is larger than previous estimates with ultraviolet/visible nadir instruments. This can be due to an initially large opacity of the plume, due to large ash and water vapor content in the early plume. Starting from end-January-February 2022, we observed a long-lasting SA plume, formed though two separate build-up phases. The plume circumnavigated the Earth rapidly (1-month time scale) and dispersed meridionally more slowly. Marked anomalies in SA OD, with respect to a 2007–2018 climatology, are observed in the tropics, for the whole year 2022, and at southern hemispheric mid- and high-latitudes starting from April 2022. Overall, a limited (∼20%) SA removal is observed after 1-year of plume dispersion. The total SA mass burden was estimated at 1.6 ± 0.5 Tg in total column, with possibly ∼40–50% in the stratosphere (∼0.65–0.80 Tg) and the remaining ∼50–60% in the troposphere (∼0.80–0.95 Tg). The build-up e-folding time of the SA plume was estimated at ∼2 months. Using the new infrared SA OD obtained with IASI and the visible AOD with OMPS-LP, we estimated a broad-band AE of ∼1.13 in March 2022, which is consistent with previous visible-only AE estimations and relatively (around 0.5 μm on average) large SA particles.

Data Availability Statement

The IMS/IASI SO_2 and SA OD daily data sets used in this work (L2 format) can be accessed through the CEDA (2023) catalog. The IMS/IASI SO_2 and SA OD daily and monthly mean data sets are available at Sellitto (2023a, 2023b). The OMPS-LP data are freely available at EarthData (2023).

Acknowledgments

This research has been supported by the Agence Nationale de la Recherche (Grant number: 21-CE01-0007-01, ASTuS), the Centre National d'Études Spatiales (CNES) via TOSCA/IASI and TOSCA/EXTRA-SAT Grants, the Centre national de la recherche scientifique-Institut National des Sciences de l'Univers (CNRS-INSU PNTS (Programme National de Télédétection Spatiale)) via MIA-SO_2 Grant. The IMS scheme development was funded by the UK National Centre for Earth Observation (NCEO, Grant numbers NE/R016518/1 and NE/N018079/1). IMS retrievals were produced using JASMIN, the UK collaborative data analysis facility, at the Rutherford Appleton Laboratory.

References

Biermann, U. M., Luo, B. P., & Peter, T. (2000). Absorption spectra and optical constants of binary and ternary solutions of H2 SO4, HNO3, and H2 O in the mid infrared at atmospheric temperatures. *Journal of Physical Chemistry-US*, *104*(4), 783–793. https://doi.org/10.1021/jp992349i

Bourassa, A. E., Robock, A., Randel, W. J., Deshler, T., Rieger, L. A., Lloyd, N. D., et al. (2012). Large volcanic aerosol load in the stratosphere linked to Asian monsoon transport. *Science*, *337*(6090), 78–81. https://doi.org/10.1126/science.1219371

Carn, S., Krotkov, N., Fisher, B., & Li, C. (2022). Out of the blue: Volcanic SO2 emissions during the 2021-2022 eruptions of Hunga Tonga - Hunga Ha'apai (Tonga). *Frontiers of Earth Science*, *10*. https://doi.org/10.3389/feart.2022.976962

Carn, S. A., Clarisse, L., & Prata, A. J. (2016). Multi-decadal satellite measurements of global volcanic degassing. *Journal of Volcanology and Geothermal Research*, *311*, 99–134. https://doi.org/10.1016/j.jvolgeores.2016.01.002

Carr, J. L., Horvath, A., Wu, D. L., & Friberg, M. D. (2022). Stereo plume height and motion retrievals for the record-setting Hunga Tonga-Hunga Ha'apai eruption of 15 January 2022. *Geophysical Research Letters*, *49*(9), e2022GL098131. https://doi.org/10.1029/2022GL098131

CEDA. (2023). CEDA catalog. [Dataset]. https://catalogue.ceda.ac.uk/uuid/489e9b2a0abd43a491d5afdd0d97c1a4

Clerbaux, C., Boynard, A., Clarisse, L., George, M., Hadji-Lazaro, J., Herbin, H., et al. (2009). Monitoring of atmospheric composition using the thermal infrared IASI/MetOp sounder. *Atmospheric Chemistry and Physics*, *9*(16), 6041–6054. https://doi.org/10.5194/acp-9-6041-2009

Clyne, M., Lamarque, J.-F., Mills, M. J., Khodri, M., Ball, W., Bekki, S., et al. (2021). Model physics and chemistry causing intermodel disagreement within the VolMIP-Tambora Interactive Stratospheric Aerosol ensemble. *Atmospheric Chemistry and Physics*, *21*(5), 3317–3343. https://doi.org/10.5194/acp-21-3317-2021

Coy, L., Newman, P. A., Wargan, K., Partyka, G., Strahan, S. E., & Pawson, S. (2022). Stratospheric circulation changes associated with the Hunga Tonga-Hunga Ha'apai Eruption. *Geophysical Research Letters*, *49*(22), e2022GL100982. https://doi.org/10.1029/2022GL100982

Duchamp, C., Wrana, F., Legras, B., Sellitto, P., Belhadji, R., & von Savigny, C. (2023). Observation of the aerosol plume from the 2022 Hunga Tonga—Hunga Ha'apai eruption with SAGE III/ISS. *Geophysical Research Letters*, *50*(18), e2023GL105076. https://doi.org/10.1029/2023GL105076

EarthData. (2023). OMPS-NPP L2 LP aerosol extinction vertical profile swath daily 3slit V2. [Dataset]. https://disc.gsfc.nasa.gov/datasets/OMPS_NPP_LP_L2_AER_DAILY_2/summary

Forster, P. M., Smith, C. J., Walsh, T., Lamb, W. F., Lamboll, R., Hauser, M., et al. (2023). Indicators of Global Climate Change 2022 annual update of large-scale indicators of the state of the climate system and human influence. *Earth System Science Data*, *15*(6), 2295–2327. https://doi.org/10.5194/essd-15-2295-2023

Guermazi, H., Sellitto, P., Cuesta, J., Eremenko, M., Lachatre, M., Mailler, S., et al. (2021). Quantitative retrieval of volcanic sulfate aerosols from IASI observations. *Remote Sensing*, *13*(9), 1808. https://doi.org/10.3390/rs13091808

Jenkins, S., Smith, C., Allen, M., & Grainger, R. (2023). Tonga eruption increases chance of temporary surface temperature anomaly above 1.5°C. *Nature Climate Change*, *13*(2), 127–129. https://doi.org/10.1038/s41558-022-01568-2

Khaykin, S., Podglajen, A., Ploeger, F., Grooß, J.-U., Tence, F., Bekki, S., et al. (2022). Global perturbation of stratospheric water and aerosol burden by Hunga eruption. *Communications Earth & Environment*, *3*(1), 316. https://doi.org/10.1038/s43247-022-00652-x

Kloss, C., Berthet, G., Sellitto, P., Ploeger, F., Taha, G., Tidiga, M., et al. (2021). Stratospheric aerosol layer perturbation caused by the 2019 Raikoke and Ulawun eruptions and their radiative forcing. *Atmospheric Chemistry and Physics*, *21*(1), 535–560. https://doi.org/10.5194/acp-21-535-2021

Kloss, C., Sellitto, P., Renard, J.-B., Baron, A., Bègue, N., Legras, B., et al. (2022). Aerosol characterization of the stratospheric plume from the volcanic eruption at Hunga Tonga 15 January 2022. *Geophysical Research Letters*, *49*(16), e2022GL099394. https://doi.org/10.1029/2022GL099394

Legras, B., Duchamp, C., Sellitto, P., Podglajen, A., Carboni, E., Siddans, R., et al. (2022). The evolution and dynamics of the Hunga Tonga–Hunga Ha'apai sulfate aerosol plume in the stratosphere. *Atmospheric Chemistry and Physics*, *22*(22), 14957–14970. https://doi.org/10.5194/acp-22-14957-2022

Millàn, L., Santee, M. L., Lambert, A., Livesey, N. J., Werner, F., Schwartz, M. J., et al. (2022). The Hunga Tonga-Hunga Ha'apai hydration of the stratosphere. *Geophysical Research Letters*, *49*(13), e2022GL099381. https://doi.org/10.1029/2022GL099381

Poli, P., & Shapiro, N. M. (2022). Rapid characterization of large volcanic eruptions: Measuring the impulse of the Hunga Tonga Ha'apai explosion FromnTeleseismic waves. *Geophysical Research Letters*, *49*(8), e2022GL098123. https://doi.org/10.1029/2022GL098123

Saunders, R., Hocking, J., Rundle, D., Rayer, P., Havemann, S., Matricardi, M., et al. (2017). RTTOV v12 science and validation report. https://www.nwpsaf.eu/site/download/documentation/rtm/docs_rttov12/rttov12_svr.pdf

Schoeberl, M. R., Wang, Y., Ueyama, R., Taha, G., Jensen, E., & Yu, W. (2022). Analysis and impact of the Hunga Tonga-Hunga Ha'apai stratospheric water vapor plume. *Geophysical Research Letters*, *49*(20), e2022GL100248. https://doi.org/10.1029/2022GL100248

Sellitto, P. (2023a). IMS/IASI SO2 total column and SA OD daily gridded data [Dataset]. *Zenodo*. https://doi.org/10.5281/zenodo.10212448

Sellitto, P. (2023b). IMS/IASI SO2 total column and SA OD monthly means gridded data [Dataset]. *Zenodo*. https://doi.org/10.5281/zenodo.10204044

Sellitto, P., Guermazi, H., Carboni, E., Siddans, R., & Burton, M. (2019). Unified quantitative observation of coexisting volcanic sulfur dioxide and sulfate aerosols using ground-based Fourier transform infrared spectroscopy. *Atmospheric Measurement Techniques*, *12*(10), 5381–5389. https://doi.org/10.5194/amt-12-5381-2019

Sellitto, P., & Legras, B. (2016). Sensitivity of thermal infrared nadir instruments to the chemical and microphysical properties of UTLS secondary sulfate aerosols. *Atmospheric Measurement Techniques*, *9*(1), 115–132. https://doi.org/10.5194/amt-9-115-2016

Sellitto, P., Podglajen, A., Belhadji, R., Boichu, M., Carboni, E., Cuesta, J., et al. (2022). The unexpected radiative impact of the Hunga Tonga eruption of 15th January 2022. *Communications Earth & Environment*, *3*(1), 288. https://doi.org/10.1038/s43247-022-00618-z

Siddans, R. (2019). Water vapor climate change initiative (WV_cci) - phase one, deliverable 2.2; version 1.0, 27 March 2019. https://climate.esa.int/documents/1337/Water_Vapour_CCI_D2.2_ATBD_Part2-IMS_L2_product_v1.0.pdf

Siddans, R. (2023). Water vapor climate change initiative (WV_cci) - phase two, ATBD Part 2 - IMS L2 product, version 2.0, 21 november 2023. https://gws-access-xp.jasmin.ac.uk/public/rsg_share/transfer/ims/Water_Vapour_CCI_D2.2_ATBD_Part2-IMS_L2_product_v2.0.pdf

Sukhodolov, T., Sheng, J.-X., Feinberg, A., Luo, B.-P., Peter, T., Revell, L., et al. (2018). Stratospheric aerosol evolution after Pinatubo simulated with a coupled size-resolved aerosol–chemistry–climate model, SOCOL-AERv1.0. *Geoscientific Model Development*, *11*(7), 2633–2647. https://doi.org/10.5194/gmd-11-2633-2018

Taha, G., Loughman, R., Colarco, P. R., Zhu, T., Thomason, L. W., & Jaross, G. (2022). Tracking the 2022 Hunga Tonga-Hunga Ha'apai aerosol cloud in the upper and middle stratosphere using space-based observations. *Geophysical Research Letters*, *49*(19), e2022GL100091. https://doi.org/10.1029/2022GL100091

Vernier, J. P., Timmreck, C., & Kremser, S. (2022). Atmospheric impacts of the 2022 Hunga Tonga-Honga Ha'apai (HT-HH) eruption. SPARC-SSiRC summary from VolRes forum postings http://www.sparc-ssirc.org/downloads/VolRes_summary_of_the_Hunga-Vfinal.pdf

Voemel, H., Evan, S., & Tully, M. (2022). Water vapor injection into the stratosphere by Hunga Tonga-Hunga Ha'apai. *Science*, *377*(6613), 1444–1447. https://doi.org/10.1126/science.abq2299

Zhu, Y., Bardeen, C. G., Tilmes, S., Mills, M. J., Wang, X., Harvey, V. L., et al. (2022). Perturbations in stratospheric aerosol evolution due to the water-rich plume of the 2022 Hunga-Tonga eruption. *Communications Earth & Environment*, *3*(1), 248. https://doi.org/10.1038/s43247-022-00580-w